Propagation of expanding ellipsoid-shaped flame

Yakun Zhang, Zifeng Weng, Rémy Mével
Center for Combustion Energy, School of Vehicle and Mobility,
State Key Laboratory of Automotive Safety and Energy, Tsinghua University
Beijing, China

1 Introduction

Spherically expanding flames have been widely used to determine laminar flame speed (S_u^0 for unburned gas, S_b^0 for burned gas), especially at elevated pressures [1]. To derive S_b^0, extrapolation relation between flame speed and stretch rate (K) should be employed. A general definition of stretch rate for a point on the surface is the Lagrangian time derivative of the area A of an infinitesimal element of the surface, $K = (1/A)(\mathrm{d}A/\mathrm{d}t)$. Due to various non-ideal effects, such as ignition [2] and chamber confinement [3], distorted flame is observed instead of the ideally spherical flame. In this case, the perimeter or area of the flame is used to obtain the equivalent flame radius [4,5]. It is noted that non-linear extrapolation relations were obtained assuming a spherical flame front. Under this assumption, stretch rate of the flame equals to the stretch due to the flame curvature (K_C) [6]. Different from non-linear relations, linear stretch relation ($S_b = S_b^0 - L_b K$, L_b is the Markstein length) was derived for arbitrary flame shapes in general fluid flows [7]. For distorted flame, another contribution for stretch rate which is caused by the non-uniform tangential velocity (K_T) should be considered. K_C and K_T can be calculated as

$$K_C = (\mathbf{v} \cdot \mathbf{n})(\nabla \cdot \mathbf{n}), \tag{1}$$

$$K_T = -\nabla \times (\mathbf{V_f} \times \mathbf{n}) \cdot \mathbf{n}, \tag{2}$$

where $\mathbf{v}$ is the velocity of the flame surface, $\mathbf{n}$ is the unit normal vector of the flame surface, and $\mathbf{V_f}$ is the tangential component of the fluid velocity at the flame front. Total stretch rate is the sum of two stretch rates, $K = K_C + K_T$. In addition, the dependence of flame speeds to two stretch rate might be different depending on the situation. Two distinct Markstein lengths were identified theoretically by asymptotic analyses [8, 9] and experimentally using the flame–vortex interaction burner [10]: one characterizes the dependence of the flame speed to stretch (referred to as the stretch Markstein length L_K) and the other one to curvature (referred to as the curvature Markstein length L_κ). Linear expression can be written as

$$S_b = S_b^0 - L_K K - S_b^0 L_\kappa K_C. \tag{3}$$

In the present study, we investigated the flame propagation initiated through an ellipsoidal flame kernel. Contributions of the flame curvature and the tangential flow to the total stretch rate were predicted for the expanding ellipsoidal flame during flame propagation. Effects of the initial shape of the flame kernel, and synthetic flame properties were also explored. In section 2, the numerical methods for predicting flame evolution are introduced and laminar flame properties are defined. In section 3, simulation results are presented and various effects on non-ideal flame propagation are discussed.

Correspondence to: mevel@mail.tsinghua.edu.cn

2 Methods

Disk-shaped flame kernel initiated by non-intrusive laser beam was observed by Susa et al. [2] using a shock tube with end-wall and side-wall imaging system, see Figure 1. From their experimental observation, the flames appear nearly identical in both the end-wall and side-wall views. Therefore, two-dimensional simulation was enough to investigate the flame evolution in the present study instead of the three-dimensional simulation. In order to deviate from ideal spherical flame, ellipsoidal flame kernel was assumed, shown in the left plot of Figure 2. Due to the the symmetrical characteristic of the propagating flame, only a quarter of the flame front in first quadrant was explored. The included angle between velocity of the surface **v** and normal vector **n** of corresponding curved front is σ. The intersections of initial ellipse and the x and y axes are (a_0,0) and (0,b_0). Based on the reported flame propagation data reported by Susa et al. [2] and flame kernel started by electric spark [11], a_0 was fixed at 4.0 mm and b_0 was varied in the range 2.0-4.0 mm. For any point on the flame surface, K is calculated based on the area change around the flame circumference, see the right plot of Figure 2.

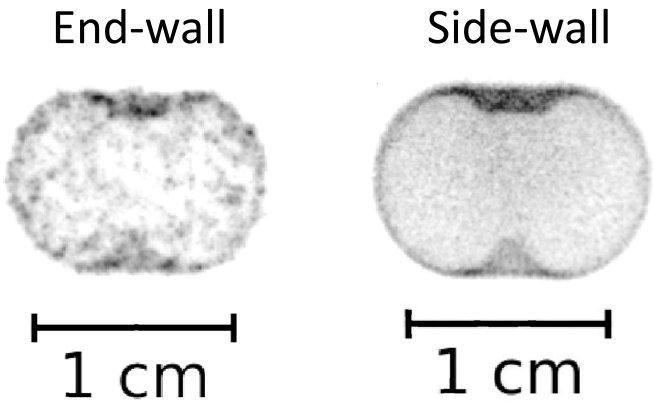

Figure 1: Sketches of disk-shaped flame from end-wall and side-wall imaging systems recorded 1 ms after the spark during a static experiment in the shock tube, see [2] for detailed information. Condition: T_u=296 K, P_u=50 kPa, propane-air mixture with equivalence ratio of 0.98.

Linear stretch relation, referred to as $S_b = f(K)$ relation, was used to predict flame propagation. Laminar flame properties, S_b^0 and L_b, are selected based on the summary of experimental measurements of these properties for various fuel–air mixtures, S_b^0 ∈[0.5,25] m/s and L_b ∈ [-3,3.5] mm. Details of this selection can be found in [12]. Furthermore, two patterns for flame propagation were defined. The first pattern is characterized by: the two intersections of flame surface with the x and y axes propagate based on the linear relation while the flame surface remains elliptic. This pattern is called axis-point propagation (AP). The second pattern is characterized by: that all the points in the surface except for the two intersections propagate based on the linear relation, which is referred to as surface propagation (SP). The two intersections are not considered for SP since the corresponding **n** is parallel to the x or y axis, which leads to $(\nabla \cdot \mathbf{n})$ equals to zero, and thus K_C equals zero. The main focus of the current work is on the SP pattern. The reason for setting the AP case was to compare with SP to check the evolution of the shape of the flame through comparison with the corresponding ellipse. Predictions of the flame evolution are implemented using MATLAB. The SP code was tested for spherical flame first to see if the $K = K_C$ was recovered and the flame speed is the same for every point on the flame surface.

Simulation steps are described as follow. First, the initial shape of the elliptic flame, the time step (dt),

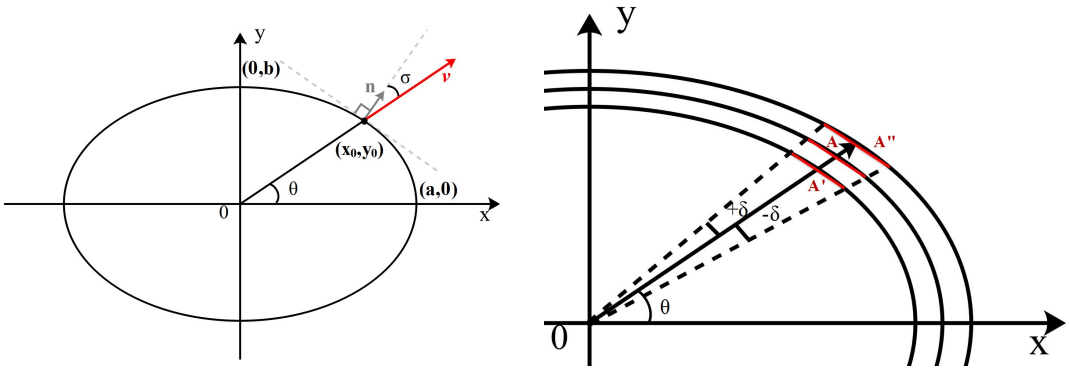

Figure 2: Diagrams of the ellipsoid-shaped flame. Left: Initial flame kernel. Right: Flame propagation and total stretch rate calculation, $K = (1/A)((A'' - A')/(t_{A''} - t_{A'}))$.

S_b^0 and L_b are specified. Then, during the first time step, very small distances (δa and δb) are added to the intersections of the initial elliptical front with the x-axis and y-axis to form the initial following flame front. The flame surface keeps its initial elliptical shape during this step. In this case, K and K_C can be calculated based on the two first flame fronts. After this first time step, the flame propagates following the $S_b = f(K)$ relation. The points on the flame surface at different time were obtained. Then, S_b, K, K_C, and K_T can be calculated based on the evolution of flame surface. The effect of the initial disturbance was eliminated by deleting data before t = 10dt since the flame shape is similar to the initial ellipse during the period $t <$ 10dt when dt is very small.

3 Results and Discussion

3.1 Comparisons between spherical flame and non-spherical flame

The difference between spherical and non-spherical flame mainly manifests through K_T. Flame propagation evolution started from an ellipsoidal kernel are shown in the left of Figure 3. The distance between AP and SP at different θ is also shown in the right plot of Figure 3. With flame expanding outwardly, it can be observed that flame shape is not perfectly elliptical for SP. However, the predictions of these two propagation patterns are similar with absolute difference at various θ below 0.1 mm at t of 5 ms. In Figure 3, the propagation speed of SP is a bit lower than that of AP. The relative positions of two predicted flame surfaces may be opposite, depending on the setting of initial conditions.

Dependencies of flame speed on K_C and K_T corresponding to the propagating process in Figure 3 for different θ are shown in Figure 4. It can be expected that K_C is decreasing as the flame propagates and this decreasing trend is the same for spherically expanding flame. It is noted that K_T for each point on the flame front decreases gradually to zero. However, K_T cannot be ignored during the early stages after ignition, especially for point close to the intersection with the x or y axes. In this case, impact brought by non-ideal flame kernel should be considered which means that it is not a correct method to use the perimeter or area of the flame to obtain the equivalent flame radius. According to the profile of K_T with time, three regions can be identified, see Figure 5. For points in region 1, K_T is negative during the whole propagation process. On the contrary, K_T is positive for points in region 3. For region 2, K_T changes sign. This change is presented in the right plot of Figure 5. The initial conditions (synthetic flame properties and flame kernel shape) significantly influence the positions of these three regions. To summarize, as the flame propagates outwardly, the effect of non-ideal tangential flow would become smaller and smaller. Flame evolution data in the quasi-steady propagating stage should be used for

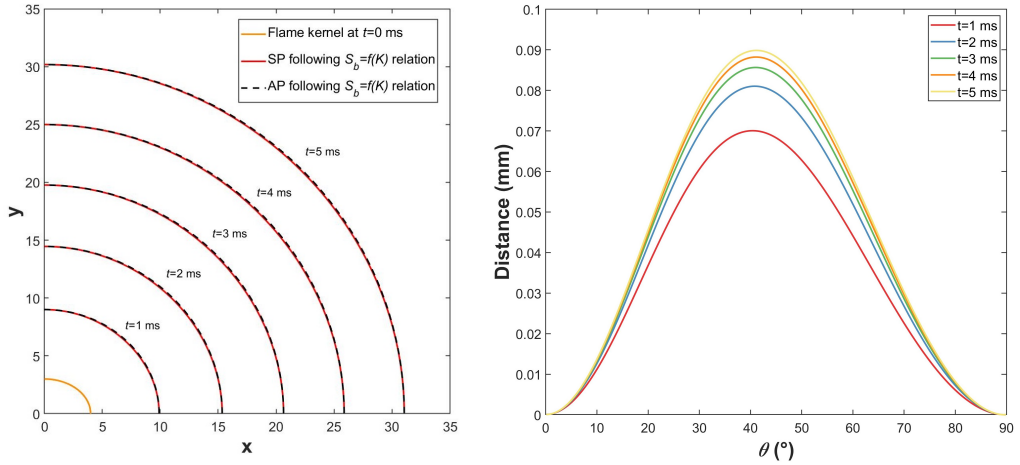

Figure 3: Flame front evolutions with time started from an elliptical kernel (left) and the distance between flame front at different θ (right) for two propagating patterns. Conditions: S_b^0=5 m/s, L_b=-0.5 mm, dt=1E-6 s, a_0=4 mm, b_0=3 mm.

laminar flame speed extrapolation since less perturbation caused by ignition exist this regime. However, flame instability would lead to the formation of cellular flame, especially under elevated pressure [13]. With limited data points available, further theoretical analysis is needed to capture the flame propagation behavior for non-spherical flame.

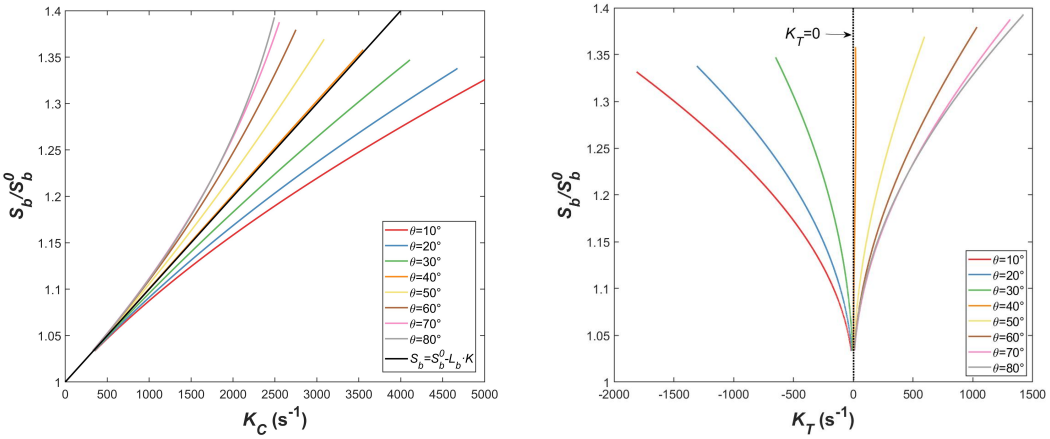

Figure 4: S_b-K_C (left) and S_b-K_T (right) relations predicted by SP pattern during flame propagation at different θ. Conditions: S_b^0=5 m/s, L_b=-0.5 mm, dt=1E-6 s, a_0=4 mm, b_0=3 mm.

3.2 Effect of the flame kernel shape

The effect of various flame kernel is shown in Figure 6. The parameter a_0 was fixed at 4 mm, while b_0 was varied from 2 mm to 3.5 mm. For various flame kernel shape, K_T is always decreasing as the flame propagating outwardly, and when the flame radius is large enough, tangential flow has little effect. However, it can be seen that the eccentricity of initial ellipse has a great impact on the evolution of K_T. In general, if the eccentricity of flame kernel is larger, which means that the shape of the flame kernel deviates more from the ideal spherical, the effect of K_T is more significant. For example, K_T could be

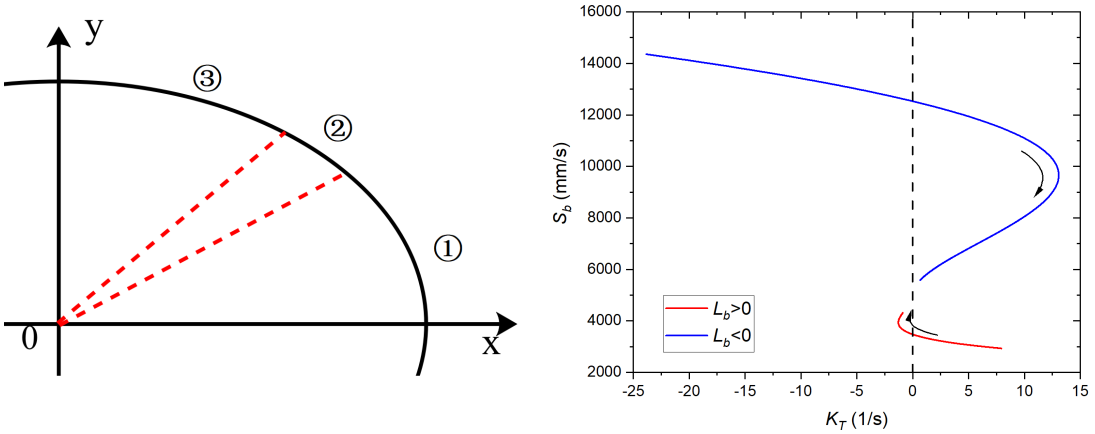

Figure 5: Three regions for the flame surface distinguished by different S_b-K_T relation (left) and relationship between flame speed and K_T for region 2 (right).

larger than K_C within the first ms after the flame kernel starts to expand for points near the x or y axes. Such a result is related to that the included large value of the angle between the propagating velocity vector and the normal vector of the flame surface.

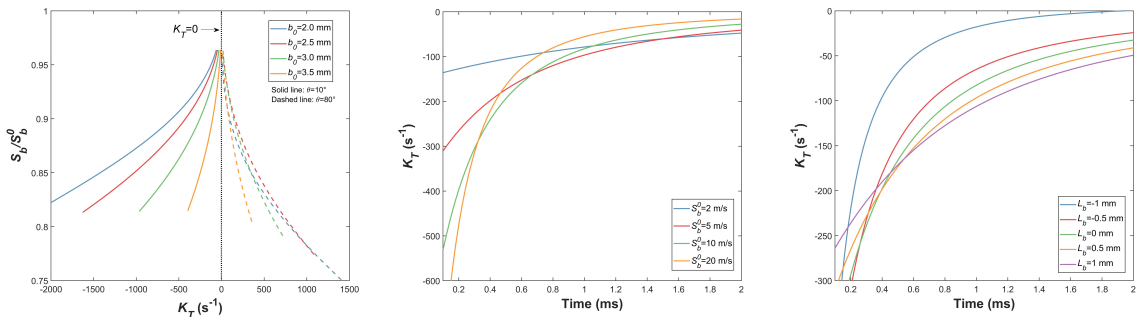

Figure 6: Evolution of K_T for different elliptical flame kernel (left), unstretched laminar flame speed for burned gas in LS relation (middle), and Markstein length in LS relation (right). Conditions: (left) a_0=4 mm, S_b^0=5 m/s, L_b=0.5 mm, θ=10/80°; (middle) a_0=4 mm, b_0=3 mm, L_b=0.5 mm, θ=30°; (right) a_0=4 mm, b_0=3 mm, S_b^0=5 m/s, θ=30°.

3.3 Effects of the synthetic laminar flame properties

The effects of laminar flame properties selected for the linear stretch relation, S_b^0 and L_b, on evolution of K_T with time are shown in the middle and right plots of Figure 6. For studying the effect of S_b^0, L_b was set at 0.5 mm. For studying the effect of L_b, S_b^0 was set at 5 m/s. It is noteworthy that, at early stage of propagation, K_T is increasing with S_b^0. However, the faster the flame speed is, the faster the value of K_T approaches zero. Similar results were observed for different Markstein length values. For more negative L_b, the effect of tangential strain is more significant at the beginning of flame expansion. The absolute value of K_T declines more rapidly for negative L_b than that of positive L_b. These results are valid for all the points on the flame surface. For a fixed stretch rate, when S_b^0 is larger under a specified L_b or L_b is smaller under a specified S_b^0, S_b turns out to be larger. The impact brought by the non-ideal flame kernel can be quickly reduced if the propagation speed of the flame surface is larger. This result is consistent with the expansion process described in the two previous subsections. After initial flame

kernel formation, the larger absolute value of K_T for higher S_b^0 and lower L_b is related to the uneven flame propagation along the flame surface. In the middle plot of Figure 6, the flame speed difference between the points near the x and y axes is large, which could strengthen the influence of the initial non-ideal kernel shape. In the right plot of Figure 6, it is seen that the effect of tangential flow vary a lot for negative L_b at t <0.2 ms.

3 Conclusion

We studied the propagation of expanding ellipsoid-shaped flame initiated from an ellipsoidal flame kernel through numerical simulation of synthetic flame. Linear stretch relation was employed to predict the flame front evolution since it is valid for arbitrary flame shapes in general fluid flows. Dependencies of flame speeds to two stretch rates, curvature stretch K_C and tangential stretch K_T, are different for ellipsoid-shaped flame. Effect of non-spherical flame kernel manifests itself by tangential stretch. As the flame expands outwardly, K_T decreases gradually to zero and K_C gets closer to the total stretch rate. According to different S_b-K_T relations, three regions on the flame surface can be identified. At early stage of flame propagation, the shape of the flame kernel and laminar flame properties of the reactive mixture have great impacts on the tangential stretch effect. The present results imply that data of large flame radius should be used for laminar flame speed extrapolation. However, some other perturbation sources would limit the available flame data. Further theoretical analysis and experimental measurement are needed to capture propagation process for non-ideal expanding flame.

References

[1] Egolfopoulos FN, Hansen N, Ju Y, Kohse-Hoinghaus K, Law CK, Qi F. (2014). Prog. Energy Combust. Sci. 43:36.

[2] Susa AJ, Hanson RK. (2022). Combust. Flame. 237: 111842.

[3] Burke MP, Chen Z, Ju Y, Dryer FL. (2009). Combust. Flame. 1567: 771.

[4] Mével R, Lafosse F, Chaumeix N, Dupré G, Paillard C. (2009). Int. J. Hydrogen Energy. 34: 9007.

[5] Goulier J, Chaumeix N, Halter F, Meynet N, Bentaïb A. (2017). Nucl. Eng. Technol. 312: 217.

[6] Chung SH, Law CK. (1984). Combust. Flame. 55: 123.

[7] Matalon M, Matkowsky B. (1982). J. Fluid Mech. 124: 239.

[8] Bechtold JK, Matalon M. (2001). Combust. Flame. 127: 1906.

[9] Clavin P, Grana-Otero JC. (2011). J. Fluid Mech. 686: 187.

[10] Thiesset F, Halter F, Bariki C, Lapeyre C, Chauveau C, Gökalp I, Selle L, Poinsot T. (2017). J. Fluid Mech. 831: 618.

[11] Halter F, Chen Z, Dayma G, Bariki C, Wang Y, Dagaut P, Chauveau C. (2020). Combust. Flame. 212: 165.

[12] Zhang Y, Coronel SA, Mevel R. (2022). Fuel. 310: 122367.

[13] Matalon M. (2009). Proc. Combust. Inst. 32: 57.